Capacitive malaria aptasensor using *Plasmodium falciparum* glutamate dehydrogenase as target antigen in undiluted human serum.

Naveen K. Singh[1], Sunil K. Arya[2,+], Pedro Estrela[2*] and Pranab Goswami[1*]

[1] Department of Biosciences and Bioengineering, Indian Institute of Technology Guwahati, Pin: 781039 Assam, India.

[2] Centre for Biosensors, Bioelectronics and Biodevices (C3Bio) and Department of Electronic and Electrical Engineering, University of Bath, Claverton Down, Bath BA2 7AY, United Kingdom.

[+] Current address: Gwent Electronic Materials Ltd, Monmouth House, Mamhilad Park, Pontypool, Torfaen NP4 0HZ. United Kingdom

***Correspondence:** 1. Fax: +91 361 2582249; Tel: +91 361 2582202; E-mail: pgoswami@iitg.ernet.in (P. Goswami)

2. Tel.: +44-1225-386324; E-mail: p.estrela@bath.ac.uk (P. Estrela)

Abstract

A highly sensitive and selective capacitive aptasensor for detecting the malaria biomarker, *Plasmodium falciparum* glutamate dehydrogenase (*Pf*GDH), directly in human serum samples is reported here. A thiolated ssDNA aptamer (NG3) that binds specifically to *Pf*GDH with high affinity (K_d = 79 nM) was developed through a SELEX procedure. The aptamer was used for the development of an aptasensor against *Pf*GDH using a non-Faradaic electrochemical impedance based signal transduction technique by monitoring the capacitance response at a frequency of 2 Hz. The aptasensor exhibited a wide dynamic range of 100 fM - 100 nM. The limits of detection obtained for the aptasensor were 0.43 pM in buffer and 0.77 pM in serum samples. Significantly low interferences from other predominant malarial biomarkers, namely, *Plasmodium falciparum* –lactate dehydrogenase and -histidine rich protein-II spiked serum samples were displayed by the aptasensor. This *Pf*GDH aptasensor with highly sensitive and label free detection capability has great application potential for diagnosis of asymptotic malaria and monitoring the regression of malaria during treatment regime with antimalarial drugs.

Keywords- Aptamer, Biosensor, Capacitance, Surface plasmon resonance, *Pf*GDH, Malaria.

Introduction

Malaria is an infectious disease that occurs mostly in tropical and sub-tropical regions of the planet (Margaret et al., 2017). The World Health Organization (WHO) reported that half of the total malaria related deaths occurred in the year 2015 were caused solely by the infection of the *Plasmodium falciparum* species (World Health Organization, 2016). Malaria is a curable disease provided an appropriate diagnosis and linked follow-up treatment for the suspected persons are offered on time. Till date microscopic investigation is considered as the gold standard method for malaria diagnosis. Several other methods such as ELISA, buffy coat analysis, nucleic acid amplification and rapid diagnostic test (RDT) are also utilized and show good sensitivity (Tangpukdee et al., 2009). However, all these methods, except RDTs, are difficult to employ in point of care (POC) settings and resource limited environments due to requirement of expensive equipment and skilled operators (Morassin et al., 2002). Most of the RDTs for malaria employed in POC are antibody based and thus, have their own sets of limitations such as poor stability in hot and humid climates, exhibit variable results and do not offer quantification of parasitic load, which could lead to misdiagnosis (Jorgensen et. al., 2006, Erdman and Kain, 2008).

Over the last decade, aptamers are evolved as potential next generation biorecognition molecules for analytical applications. Nucleic acid aptamers are short chain oligonucleotides which can bind to a target molecule with high selectivity and sensitivity. ssDNA aptamers offer several advantages over antibodies such as ease of large scale production at low cost following *in vitro* chemical protocol, high thermal stability and long shelf-life, compatible chemistry to immobilize over sensor surfaces and scope to enhance their performance factors through chemical modifications (Kakoti and Goswami 2017; Cheung et al., 2013).

For malaria diagnosis, various biomarker proteins like lactate dehydrogenase (LDH), histidine rich protein (HRP-II), aldolase, and glutamate dehydrogenase have been explored

(Jain et al., 2014). Most of the RDTs available for the detection of *Plasmodium falciparum* (*Pf*) are based on *Pf*HRP-II as the target antigen. However, reports claim that there are deletions of the *Pf*HRP-II gene in some of the African and Asian regions (Murillo et al., 2015; Viana et al., 2017), which prompted to explore other available biomarkers for developing reliable detection device for the parasite *Plasmodium falciparum*. The *Plasmodium falciparum* glutamate dehydrogenase (*Pf*GDH) is recognised as a powerful malaria biomarker as it is considerably different from the host GDH in terms of structure, sequence, location and enzyme kinetics (Werner et al., 2005; Zaganas et al., 2009). It is present only in detectable amounts in the serum of *Plasmodium falciparum* infected patients (Li et al., 2005; Seol et al., 2017).

Electrochemical impedance spectroscopy (EIS), either in Faradaic or non-Faradaic modes, has recently received enormous interest in the field of biosensors due to its highly sensitive signal transduction feature (Wang et al., 2017; Rohrbach et al., 2012). In non-Faradaic EIS measurements, variations in interfacial capacitance developed by dislocating water molecules and ions away from a bio-functionalised electrode surface after its binding to the target molecule is used for sensor application (Tkac and Davis, 2009). Furthermore, non-Faradaic EIS measurements are label-free, simple, and direct allowing the measurement of the target molecule in undiluted serum making it suitable for point of care applications (Arya et al., 2018, Luo et al., 2013).

Herein, a *Pf*GDH ssDNA aptamer selected through systemic evaluation of ligand exponential enrichment (SELEX) process was immobilized chemically over an electrode surface through a self-assembled technique. The developed aptasensor was then utilized for detecting *Pf*GDH directly in serum samples using non-Faradaic EIS technique. The aptasensor shows great sensitivity, specificity and dynamic range

Materials and Methods

Materials

Dibasic/mono basic phosphate buffer, $MgCl_2$, NaCl, KCl, alumina powder (50 nm coarse size), PCR kit, streptavidin magnetic beads, human serum albumin (HSA) and human serum from AB positive male were procured from Sigma Aldrich. Starting blocking buffer, H_2SO_4 and Top 10 competent cells were procured from Thermo Fisher. The single stranded random N40 oligonucleotide DNA library with conserved primer binding site and primer were received from IDT technology (USA). All the proteins (*Pf*GDH, HGDH, *Pf*LDH and *Pf*HRP-II) used in the present investigation were previously cloned, expressed and characterised in house (Chakma et al., 2016; Goswami et al., 2016; Jain et al., 2016). Thiolated HPLC grade purified *Pf*GDH aptamer NG3 and NG51 (see Table 1) were obtained from Sigma (UK).

Table 1. Thiolated NG3 and NG51 aptamer sequences.

Aptamer	Sequences (5'→3')
NG3	SH-$(CH_2)_6$-TTT TCA CCT CAT ACG ACT CAC TAT AGC GGA TCC GAG CCG GGG TGT TCT GTT GGC GGG GGC GGT GGG CGG GCT GGC TCG AAC AAG CTT GC
NG51	SH-$(CH_2)_6$-TTT TCA CCT CAT ACG ACT CAC TAT AGC GGA CCC CAC TCA CTG CTC GGA CTC TCC CCC TCC CCG CCT GGC TCG AAC AAG CTT GC

Aptamer selection and screening

The development of the aptamer against *Pf*GDH was done through SELEX process. The ssDNA aptamer was developed from random oligonucleotide library in which a random 40-nucleotide region (Fw-N40-Rev) was flanked by conserved primer binding site for amplification. A polyvinylidene difluoride (PVDF) membrane was used for *Pf*GDH immobilization. Probable aptamer candidates were cloned at the end of 17 rounds of SELEX

into pGEMT easy vector and transformed into *E.coli* DH5α cells. The transform cells were selected by blue-white screening and restriction digestion. The positive clone was sequenced and the secondary structure was predicted through Mfold online software (Zuker, 2003).

Aptamer binding affinity measurement

A surface plasmon resonance (SPR) study was performed for the measurement of the dissociation constant (K_d value) of the developed aptamer against *Pf*GDH using a Reichert SPR 7000DC (USA) dual channel flow spectrophotometer at 25 °C over 50 nm gold coated chips (Reichert Technology, USA). The SPR chip was first cleaned with piranha solution (3:1 H_2SO_4: H_2O_2) for 20 s, then washed with milli-Q water (18.2 MΩ.cm, Millipore, UK) for 5 min followed by purging with N_2 gas jet for drying. The chip was then incubated overnight with thiolated aptamer (1 µM) along with 6-mercapto 1-hexanol (MCH, Sigma) in a ratio of 1:100 in binding buffer, followed by backfilling the surface with 1 mM MCH for 1 h (Aliakbarinodehi et al., 2017; Green et al., 2000). All the protein solutions and buffer were filtered through a 0.2 µm filter and degassed for 2 h. After obtaining a stable buffer SPR line, different concentrations of *Pf*GDH and control protein were flowed over the aptamer modified SPR chip at 25 µl/min for 10 minutes, followed by 5 min of a dissociation step with buffer to remove any unbound proteins.

Sensor fabrication

Bare gold disc electrodes of 3 mm diameter (CHI Instruments, USA) were cleaned with piranha solution (3:1 ratio of H_2SO_4: H_2O_2) for 30 s, followed by mechanical polishing with 50 nm course size alumina slurry (Sigma) for 5 min over a polishing pad (BASi, USA). The electrodes were then sonicated in absolute ethanol and milli-Q water for 5 min each, sequentially. Thereafter electrodes were electrochemically cleaned in 0.5 M H_2SO_4 by cycling the potential between -0.5 and +1.3 V *versus* Hg/Hg_2SO_4 till a stable characteristic reduction

current peak of bare gold was observed. The electrodes were rinsed with ample amounts of milli-Q water and then dried in N_2 gas jet steam.

The aptamers were then grafted to the clean gold electrodes following a previously reported method (Jolly et al., 2017). In brief, 100 mM of MCH was first prepared in absolute ethanol as stock solution and then diluted to 1 mM in binding buffer (10 mM potassium phosphate buffer pH 8.0 with 5 mM NaCl, 5 mM KCl and 2.5 mM $MgCl_2$). The aptamer was heat treated at 90 °C for 5 min then cooled down to room temperature (RT) for 15 min before initiating the sensor fabrication. The clean electrodes were incubated in 200 µl of *Pf*GDH specific aptamer: MCH in a 1:100 ratio and left overnight in a humidity chamber. After immobilization, the electrodes were rinsed with milli-Q water to remove unbound aptamers. To ensure proper coverage, the electrodes were further treated with 1 mM MCH for 1 h. The electrodes were again washed with milli-Q water and dried with N_2 steam and blocked with starting blocking buffer (Thermo Fisher, UK) for 30 minutes to prevent non-specific attachment of proteins over the electrodes.

EIS measurement.

Non-Faradaic EIS measurements were performed using a µAutolab III / FRA2 potentiostat (Metrohm) in a two-electrode setup consisting of aptamer functionalised gold disc electrode as working electrode and Ag/AgCl as reference electrode. The measurements were performed in binding buffer, applying a 10 mV a.c. amplitude voltage in the frequency range 1 MHz to 100 mHz. After obtaining a stable signal in the measurement buffer, the electrodes were incubated with varying concentrations of *Pf*GDH protein in 200 µl binding buffer for 30 min, following which the EIS spectra were recorded after washing the electrodes with buffer. The specificity of developed aptasensor was tested with other malaria biomarker proteins such as *Plasmodium falciparum* lactate dehydrogenase (*Pf*LDH), *Plasmodium falciparum* histidine

rich protein-II (*Pf*HRP-II) and analogous human glutamate dehydrogenase (HGDH) and HSA.

Results and Discussion

Aptamer screening and characterization

The single stranded DNA aptamer for *Pf*GDH was selected from a 10^{14-15} random ssDNA oligonucleotide library through SELEX procedure. The PVDF membrane was used as the matrix support during the SELEX procedure for protein immobilization. The protein molecule was attached in a random orientation via integration of dipole and hydrophobic interactions over the PVDF membrane (Matsudaira, 1987), which provides multiple aptatope surface for aptamer binding (Jain et al., 2016). For the selection of aptamer, a total of 17 rounds of SELEX cycle were performed, of which 3 counter SELEX cycle against PVDF membrane and 2 rounds of negative SELEX cycle with HGDH were performed to eliminate non-specific aptamers candidates (Figure 1). After the final round of PCR amplification of the isolated ssDNA candidate from the SELEX cycle, the amplicons were cloned, sequenced and aligned through Clustal X software. The alignment results showed that some sequences were enriched more during the process and out of those two candidates (NG3, NG51) with highest enrichment were finally selected (Supplementary Information, Figure S1). The secondary structures of the aptamers NG3, NG51 were determined by Mfold (Figure 2).

The selected 5’ end thiol modified aptamers were immobilized (~200 nmol) over SPR chips followed by backfilling / blocking with MCH. The prepared electrodes were then utilized for detection of different concentration of *Pf*GDH and other non-specific proteins. The binding of *Pf*GDH over the gold chip surface led to an increase in SPR angle, reaching a stabilization plateau within less than 10 mins. After binding, buffer solution was passed over the surface to remove loosely bound protein from the surface. The amount of *Pf*GDH attached to the SPR

chip was calculated by recording the difference between the final and initial SPR angle (Figure 1A, B). The specificities of the developed aptamers were analysed by testing control proteins (HGDH, *Pf*LDH, HSA), which showed negligible changes in SPR angle for both the NG3 and NG51 aptamers (Supplementary Information, Figure S2). The binding affinities of the developed aptamers were calculated using the single ligand binding site equation in 1:1 interaction mode, X+Y=XY, where X is injected target protein and Y is immobilized aptamer molecule, XY is aptamer–protein complex formed over the SPR chip. The formation of aptamer–protein complex (XY) is directly proportional to the response unit (RIU) of SPR (Scarano et al., 2010). The dissociation constant (K_d) values for the aptamers were calculated using the equation $RIU=RIU_{max}*c/(K_d+c)$, where c is the protein concentration. The K_d were determined as 79.16 ± 1.58 nM and 370 ± 14.39 nM for NG3 and NG51, respectively. The Gibbs energy, $\delta G = - RT \ln K_a$, where R is the universal gas constant, T is temperature and $K_a = 1/K_d$, was also calculated for the NG3 and NG51 aptamers at 298 K and found to be - 56.9 kJ/mol and - 36.7 kJ/mol, respectively. The negative Gibbs energy values indicate the prompt interaction of *Pf*GDH with aptamer over the solid surface platform of the SPR chip, and found to be better for NG3 aptamer candidate. Based on the higher binding affinity against *Pf*GDH and lower Gibbs energy change, NG3 was considered for further study.

Sensor surface characterization

The sensor fabrication process over the bare gold electrodes was characterized by atomic force microscopy (AFM) and cyclic voltammetry (CV). The results of AFM characterization were done in continuous tapping mode. The topographic average roughness analysis using wsxm 5.0 software analysis showed gradual decrease of roughness from bare gold (1.52 nm) to aptamer modified gold electrode (1.41 nm) and blocked aptasensor electrode (1.33 nm). This was accompanied by an increase in the average height of the surface modified

electrodes, indicating the binding of aptamer and blocking reagents over the electrode (Figure 3A-C). CV was performed to investigate the layer by layer modification of the electrodes. The results depict the quasi reversible cyclic voltammogram of $[Fe(CN)_6]^{3-/4-}$ with a decrease in oxidation and reduction currents of the modified electrodes compared to the blank gold electrode (Figure 3D). The formation of a self-assembled monolayer of aptamer-MCH over the gold electrode led to an increase in ΔEp (difference between oxidation and reduction potentials) and lowered the redox current. This could be attributed to the charge repulsion caused by the negative phosphate backbone of the aptamer (Bang et al., 2005) as well as the passivation of the electrode hindering the electron transfer. The results suggest successful assembly of the aptamer over the electrode surface. After blocking of aptamer/MCH electrode with the starting blocking buffer, a further decrease in redox current was observed due to void spaces of gold and/or MCH being occupied by non-conducting moieties of the blocking buffer.

Detection of PfGDH

The NG3 aptamer was used for *Pf*GDH sensing following non-Faradaic impedance measurements without using any redox marker in the solution. In this mode, high values of impedance were observed and variations in the capacitance of the system that occurred due to the binding of the aptamer with the target protein were measured. The capacitive response of the sensor was discerned by measuring $1/\omega Z''$, where ω is the angular frequency and Z'' the imaginary part of the impedance of the system. A maximum in the phase angle was observed at ~2 Hz, indicating maximum capacitive response at this frequency (Figure 4A). This frequency was thus used for plotting the dose response of the capacitive variation signal. The reduction in capacitance with increasing concentrations of *Pf*GDH indicates successful binding of the target molecule with the NG3 aptamer (Figure 4B, C). The change in

capacitance is attributed to the alteration in dielectric properties of the biolayer through the replacement of solvated ions and water molecules by the protein, as well as due to the increase in thickness of the biolayer upon protein binding (Arya et al., 2018; Liu et al., 2017). The limit of detection (LOD) (3x standard deviation of blank/slope of calibration curve) of *Pf*GDH was found to be 0.43 pM in the buffer, with a linear (in log scale) detection range of 100 fM to 100 nM (Figure 4D).

The capacitive aptasensor was then tested directly in undiluted blood serum with spiked *Pf*GDH. The *Pf*GDH protein with different concentrations that fall within the dynamic range obtained in the buffer medium (100 fM - 100 nM) was used in the undiluted serum (Figure 5). This range covers the previously reported *Pf*GDH concentrations used (2 to 16 nM) for malaria diagnosis through an immuno-chromatographic dipstick based method (Djadid et al., 2014; Li et al., 2005). Like in buffer, a maximum phase angle was observed at ~2 Hz during the measurement of serum spiked *Pf*GDH protein (Figure 5A). The capacitance at 2 Hz was therefore considered further for plotting the calibration curve (Figure 5B). The detection in serum followed a linear dependency (in log scale) for the whole range and an LOD of 0.77 pM for *Pf*GDH was discerned (Figure 5C). The results indicate a comparable signal sensitivity of the aptasensor between samples in buffer and serum media, which validate a conducive microenvironment for the interaction of the aptamer with the target antigen protein in the serum medium (Park et al., 2012). The binding between *Pf*GDH and NG3 aptamer over electrode was probably caused by the interaction between some positively charged *Pf*GDH amino acid and negatively charged ssDNA aptamer. The net surface charge of aptamer-protein complex governed the dielectric property over the sensing surface of electrode which was not affected by the ionic microenvironment in serum in the present case (Cole and Cole, 1941; Pethig and Kell, 1987). The interferences from the other prominent malaria biomarker proteins (*Pf*LDH and HRP-II) that are likely to be secreted during the malaria condition were

examined by spiking these proteins in undiluted serum (Figure 5D). The responses were 6.5% (*Pf*LDH) and 0.5% (*Pf*HRP-II) of the control protein (*Pf*GDH) for the corresponding proteins shown in the parentheses. The results indicate only a minor non-specific interaction of the sensor with the *Pf*LDH protein. The sensitive response profile obtained directly on the serum sample indicates that the serum components including HGDH and the predominant serum protein, HSA do not significantly interfere with the aptasensor function. Hence the proposed sensor has potential to be developed as a practical sensor for malaria diagnosis.

Conclusion

Herein, a reagent-free and label-free aptasensor for diagnosis of malaria using non-Faradaic EIS has been demonstrated. This is the first report on *Pf*GDH aptasensor exploiting non-Faradaic impedance technique as signal transduction platform. A sensitive aptamer (NG3) was developed through a screening technique and rational approach. A significantly low dissociation constant (K_d=79 nM) discerned for the aptamer–*Pf*GDH interaction validates its strong binding affinity towards the target antigen. The stable chemical immobilization of the aptamer over the electrode surface through SAM approach offered additional advantages of easy and reproducible fabrication of the aptasensor. The broad detection range and ultra-low limit of detection enables the sensors to be used for diagnosis of asymptomatic malaria and monitoring the regression of malaria during treatment regime with antimalarial drugs. Overall, this simple, redox free, robust and highly sensitive non-Faradaic capacitance-based aptasensor for *Pf*GDH has great application potential for diagnosis of malaria using untreated and undiluted serum samples in POC settings.

Acknowledgements

N.K.S. acknowledges support from the DBT, India and the British Council in the form of a Newton-Bhabha PhD Placement Grant (2016-17). S.K.A. was funded by a Marie Skłodowska-Curie Individual Fellowship through the European Commission's Horizon 2020 Programme (grant no. 655176).

Figures

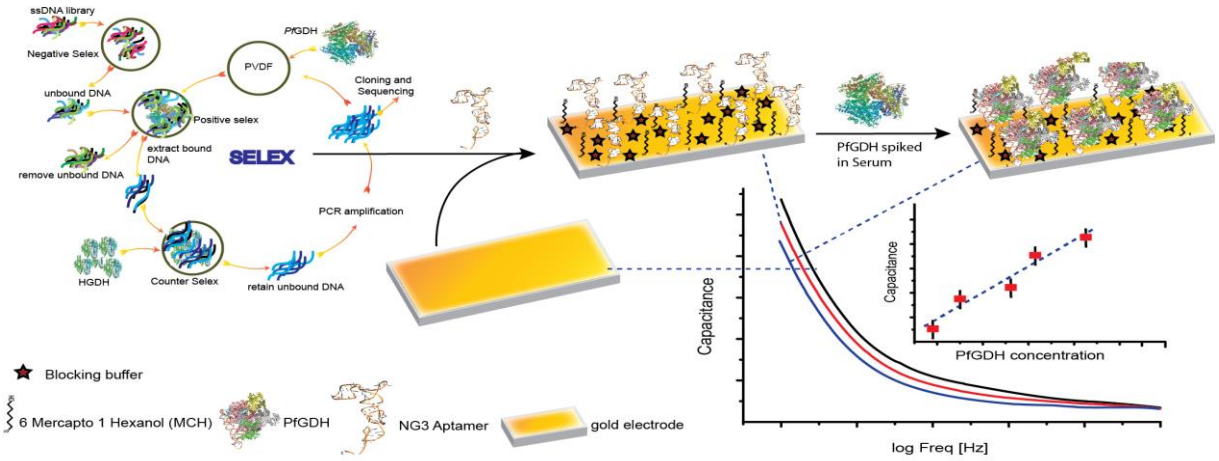

Figure 1. Fabrication of electrode with aptamer and detection of *Pf*GDH, development of aptamer through SELEX.

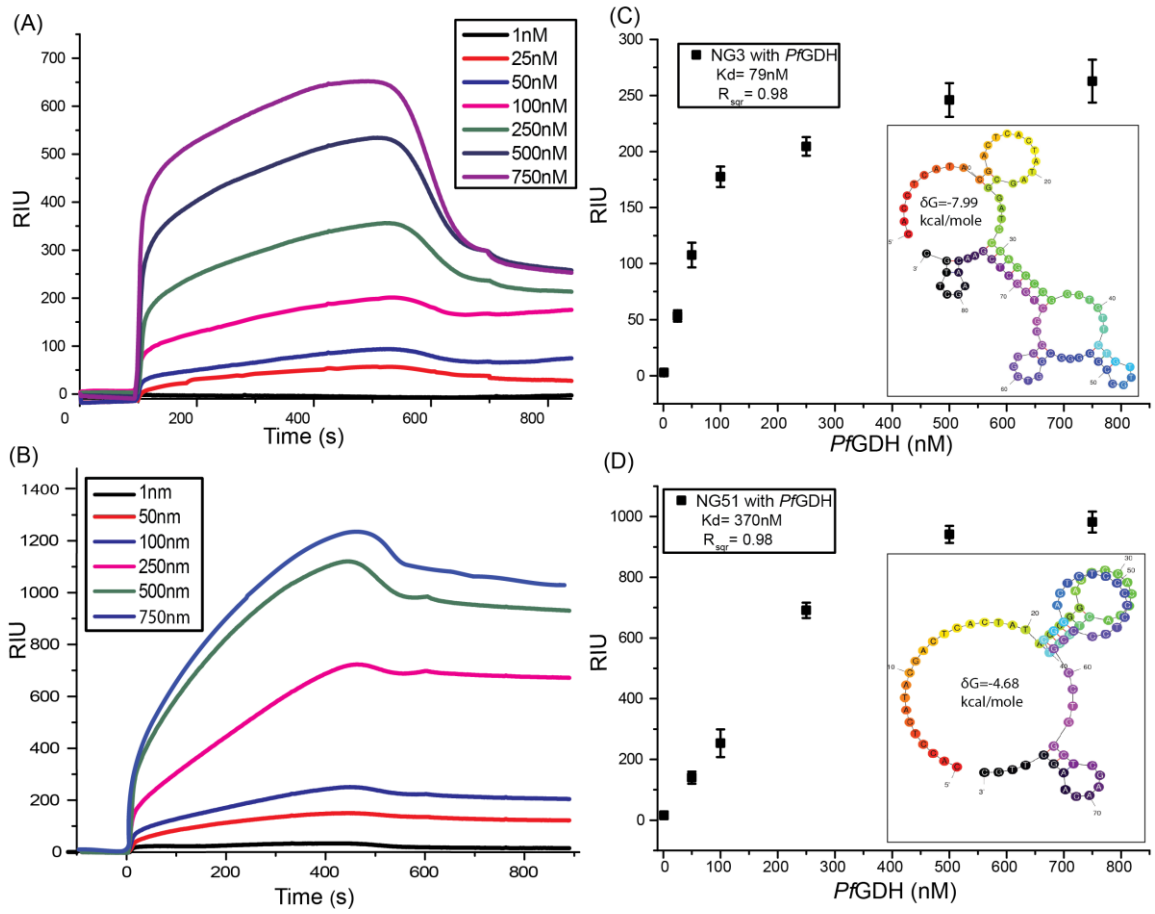

Figure 2. SPR sensogram for NG3 (A) and NG51 (B) with different concentration of *Pf*GDH. Plotting of sensogram data for determination of dissociation constant (K_d) for (C) NG3 and (D) NG51. Inset secondary structure of NG3, NG51 aptamer along with δG values.

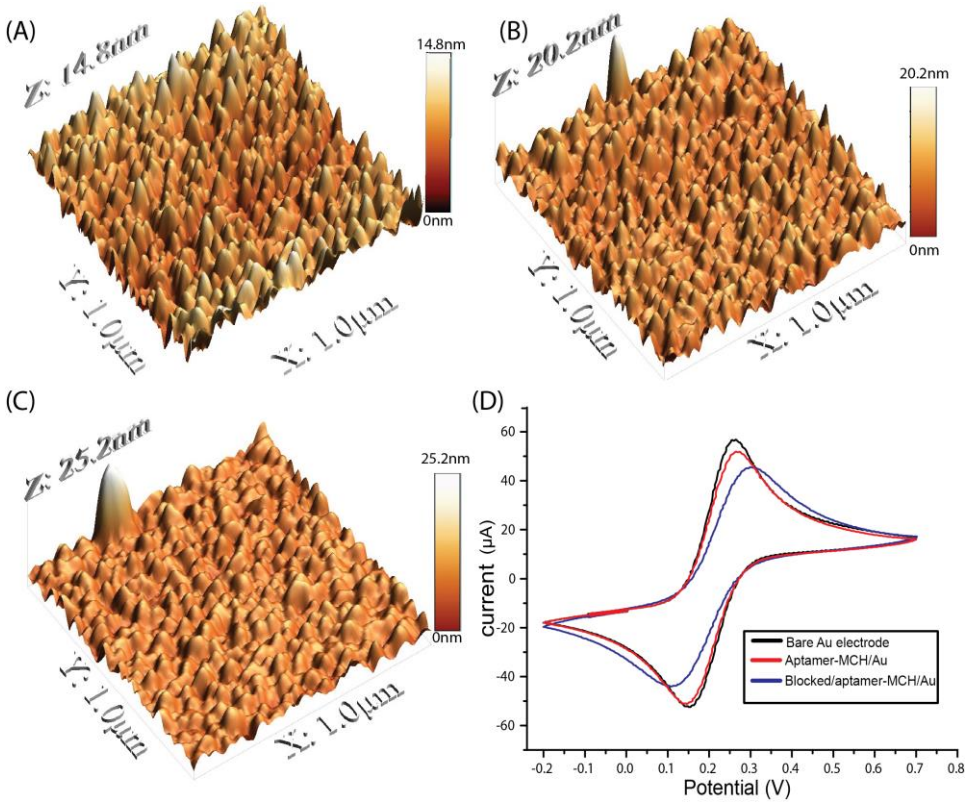

Figure 3. AFM images of (A) bare gold electrode (B) surface assembled monolayer with aptamer-MCH over gold electrode (C) surface blocking with MCH and blocking buffer over aptamer modified electrode. (D) CV of the electrodes recorded by using Ag/AgCl as reference electrode. Scan rate of 50 mV/s in 10 mM potassium hexacyanoferrate solution prepared in PBS.

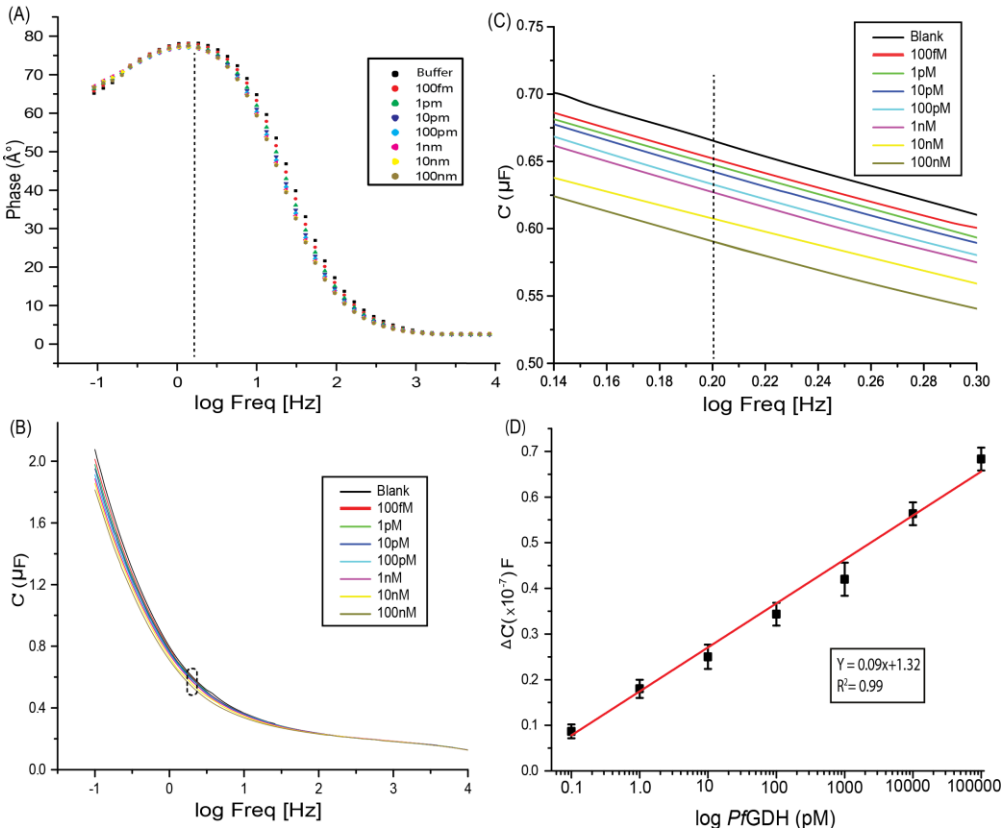

Figure 4. Non-Faradaic measurement in buffer (A) Phase response vs frequency, (B) Capacitance response of NG3 aptamer-*Pf*GDH with circled enlarged image in inset. (C) Enlarged image of circled region of capacitance responses. (D) Calibration curve of capacitance response at 2 Hz versus log *Pf*GDH concentrations spiked in buffer.

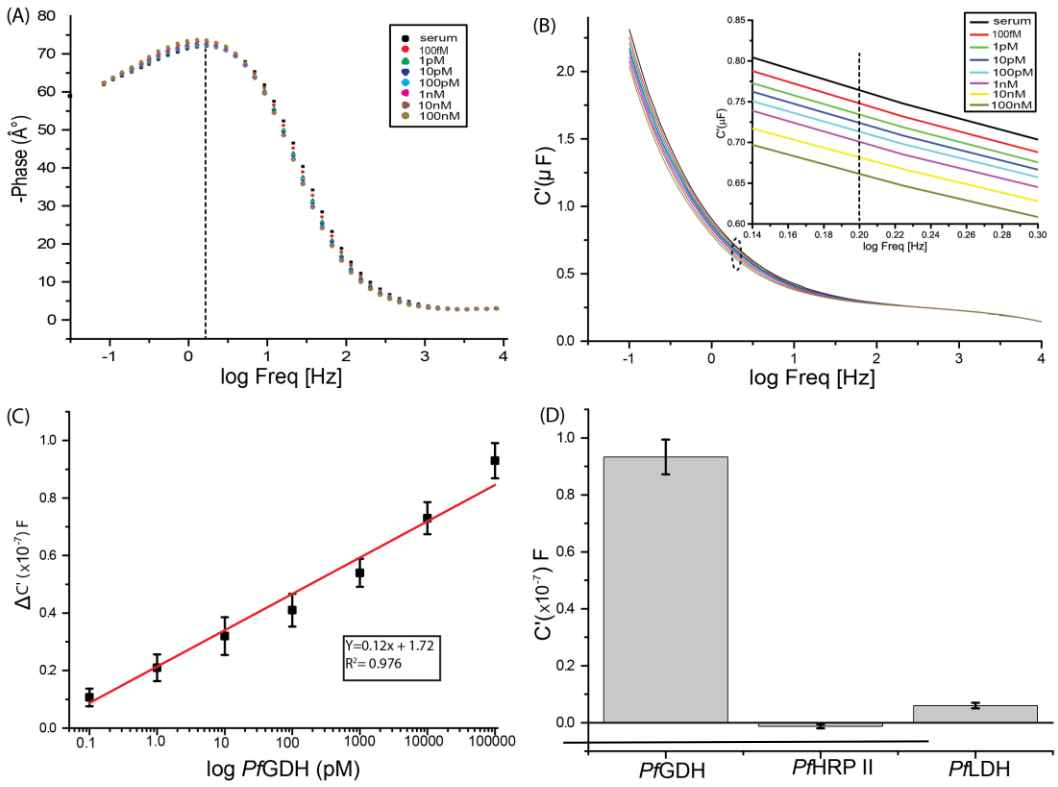

Figure 5. (A) Non-Faradaic measurement in undiluted serum Phase response vs frequency. (B) Capacitance response of NG3 aptamer-*Pf*GDH with circled enlarged image in inset. (C) Calibration curve of capacitance response at 2 Hz verses log *Pf*GDH concentrations spiked in undiluted serum. (D) Response of NG3 aptamer with analogue proteins each with 100 nM spiked in serum.

References

Aliakbarinodehi, N., Jolly, P., Bhalla, N., Miodek, A., De Micheli, G., Estrela, P., Carrara, S., 2017. Aptamer-based field-effect biosensor for tenofovir detection. Sci. Rep. 7, 44409.

Arya, S. K., Zhurauski, P., Jolly, P., Batistuti, M. R., Mulato, M., Estrela, P., 2018. Capacitive aptasensor based on interdigitated electrode for breast cancer detection in undiluted human serum. Biosens. Bioelectron. 102, 106–112.

Bang, G. S., Cho, S., Kim, B., 2005. A novel electrochemical detection method for aptamer biosensors. Biosens. Bioelectron, 21, 863–870.

Chakma, B., Jain, P., Singh, N.K., Goswami, P., 2016. Development of an indicator displacement based detection of malaria targeting HRP-II as biomarker for application in point-of-care settings. Anal. Chem. 88 (20), pp 10316–10321.

Cheung, Y. W., Kwok, J., Law, A. W. L., Watt, R. M., Kotaka, M., Tanner, J. A., 2013. Structural basis for discriminatory recognition of Plasmodium lactate dehydrogenase by a DNA aptamer. Proc. Natl. Acad. Sci. USA 110, 15967–72.

Cole, K. S., Cole, R. H., 1941. Dispersion and absorption in dielectrics I. Alternating current characteristics. J. Chem. Phys. 9 (4), 341-351.

Daniels, J. S., Pourmand, N., 2007. Label-free impedance biosensors: Opportunities and challenges. Electroanalysis, 19 (12), 1239–1257.

Djadiad, N. D., Sedighion, F., Raj, A., Zakeri, S., 2014. Gold nanoparticle based dipstick nano biosensor for detecting Plasmodium falciparum and vivax and method. US patent. US 2014/0248629 A1.

Erdman, L. K., Kain, K. C., 2008. Molecular diagnostic and surveillance tools for global malaria control. Travel Med. Infect. Dis. 6, 82–99.

Goda, T., Miyahara, Y., 2012. Molecularly engineered charge-conversion of proteins for sensitive biosensing. Langmuir 28 (41),14730–14738.

Goswami, P., Singh, N. K., Jain, P., Chakma, B., 2016. DNA aptamers specifically binding to *Plasmodium falciparum* glutamate dehydrogenase (PfGDH) Patent (Ind) application no.201631025722.

Green, R. J., Frazier, R. A., Shakesheff, K. M., Davies, M. C., Roberts, C. J., Tendler, S. J. B., 2000. Surface plasmon resonance analysis of dynamic biological interactions with biomaterials. Biomaterials 21, 1823–1835.

Jain, P., Chakma, B., Patra, S., Goswami, P., 2014. Potential biomarkers and their applications for rapid and reliable detection of malaria. Biomed Res. Int. 2014, 852645.

Jain, P., Chakma, B., Singh, N.K., Patra, S., Goswami, P., 2016. Aromatic surfactant as aggregating agent for aptamer-gold nanoparticle-based detection of *Plasmodium* lactate dehydrogenase. Mol. Biotechnol. 58 (7), 497-508.

Jorgensen, P., Chanthap, L., Rebueno, A., Tsuyuoka, R., Bell, D., 2006. Malaria rapid diagnostic tests in tropical climates: the need for a cool chain. Am. J. Trop. Med. Hyg. 74, 750–754.

Kaisti, M., 2017. Detection principles of biological and chemical FET sensors. Biosens. Bioelectron. 98, 437–448.

Li, Y., Ning, Y. S., Li, L., Peng, D. O., Dong, W. Q., Li, M., 2005. Preparation of monoclonal antibody against *Plasmodium falciparum* glutamate dehydrogenase and establishment of gold immunochromatographic assay. Di Yi Jun Yi Da Xue Xue Bao 25 (4), 435-438.

Liu, B., Lu, L., Hua, E., Jiang, S., Xie, G., 2012. Detection of the human prostate- specific antigen using an aptasensor with gold nanoparticles encapsulated by graphitized mesoporous carbon. Microchim. Acta 178, 163–170.

Liu, J., Chisti, M.M., Zeng, X., 2017. General signal amplification strategy for nonfaradic impedimetric sensing: Trastuzumab detection employing a peptide immunosensor. Anal. Chem. 89, 4013–4020.

Margaret, A. P, Jeremy, N. B., Manyando, C., van Huijsduijnen, R. H., Van Voohis, W. C., Wells, T. N. C., 2017. Malaria. Nat. Rev. Dis. Primers 3, 17050.

Matsudaira, P., 1987. Sequence from picomole quantities of proteins electroblotted onto polyvinylidene difluoride membranes. Biol. Chem. 262 (21), 10035–1003.

Morassin, B., Fabre, R., Berry, A., Magnaval, J. F., 2002. One year's experience with the polymerase chain reaction as a routine method for the diagnosis of imported malaria. Am. J.

Trop. Med. Hyg. 66, 503–508.

Murillo, S. C., Sheila, A. O., Joseph, F. A., Zuleima, P., Erika, D., Sandra. I., Curtis, S. H., Alexandre, M. O., David, B., Venkatachalam, U. K., Barnwell, J. W., 2015. Deletion of Plasmodium falciparum histidine-rich protein 2 (pfhrp2) and histidine-rich protein 3 (pfhrp3) genes in Colombian parasites. PLoS One 10 (7), e0131576.

Park, J.W., Saravan K. S., Niazi, J. H., Gurbuz, Y., Youn, B. S., Gu, M. B., 2012. Rapid and sensitive detection of Nampt (PBEF/visfatin) in human serum using an ssDNA aptamer-based capacitive biosensor. Biosens. Bioelectron. 38, 233–238.

Jolly, P., Formisano, N., Tkac, J., Kasák, P., Frost, C. G., Estrela, P., 2015. Label-free impedimetric aptasensor with antifouling surface chemistry: A prostate specific antigen case study. Sens. Actuators B 209, 306-312.

Pethig, R., Kell, D., 1987. The passive electrical properties of biological systems: their significance in physiology, biophysics and biotechnology. Phys. Med. Biol. 32, 933-970.

Rodríguez, A., Domínguez, N. G., Aguilar, I., Girón, M. E., 1998. Characterization of *Plasmodium falciparum* glutamate dehydrogenase-soluble antigen. Braz. J. Med. Biol. Res. 31, 1149–1155.

Rohrbach, F., Karadeniz, H., Erdem, A., Famulok, M., Mayer, G., 2012. Label-free impedimetric aptasensor for lysozyme detection based on carbon nanotube-modified screen-printed electrodes. Anal. Biochem. 421, 454–459.

Scarano, S., Mascinia, M., Turner, A. P. F., Minunnia, M., 2010. Surface plasmon resonance imaging for affinity-based biosensors. Biosens. Bioelectron. 25 (5), 957-966.

Seol, B., Shin, H. I., Kim, J. Y., Jeon, B. Y., Kang, Y. J., Pak, J. H., Kim, T. S., Lee, H. W., 2017. Sequence conservation of *Plasmodium vivax* glutamate dehydrogenase among Korean isolates and its application in seroepidemiology. Malar. J. 16, 3.

Tangpukdee, N., Duangdee, C., P, Wilairatana., Krudsood, S., 2009. Malaria Diagnosis: A Brief Review. Korean J Parasitol. 47 (2), 93-102.

Tkac, J., Davis, J. J., Davis, J. J., 2009. Label-free field effect protein sensing. In Davis, J. J. (ed.), Engineering the Bioelectronic Interface: Applications to Analyte Biosensing and Protein Detection. The Royal Society of Chemistry, pp. 193–224.

Trape, J. F, Pison, G., Spiegel, A., Enel, C., Rogier, C., 2002. Combating malaria in Africa, Trends Parasitol. 18, 224-30.

Viana, G. R., Akinyi, O. S, Silva, F. L, Lima, B. D, Macedo, O. A, Goldman, I. F., 2017. Histidine-rich protein 2 (*pfhrp2*) and *pfhrp3* gene deletions in *Plasmodium falciparum* isolates from select sites in Brazil and Bolivia. PLoS ONE 12 (3), e0171150.

Wagner, J. T., Lüdemann, H., Färber, P. M., Lottspeich, F., Krauth, S. R., 1998. Glutamate dehydrogenase, the marker protein of *Plasmodium falciparum* cloning, expression and characterization of the malarial enzyme. Eur. J. Biochem, 258, 813-819.

Wang, L., Veselinovic, M., Yang, L., Geiss, B. J., Dandy, D. S., Chen, T., 2017. A sensitive DNA capacitive biosensor using interdigitated electrodes. Biosens. and Bioel, 87, 646-653.

World Health Organization, 2016. World Malaria Report 2016. World Health Organization: Geneva. Available from http://www.who.int/malaria/publications/world-malaria-report-2016/report/en/; assessed April 2018.

Zaganas, I., Spanaki, C., Plaitakis, A., 2012. Expression of human GLUD2 glutamate dehydrogenase in human tissues: Functional implications. Neurochem. Int. 61, 455–462.

Zuker, M., 2003. Mfold web server for nucleic acid folding and hybridization prediction. Nucleic Acids Res. 31, 3406–3415